

## Research Paper

## Micro mechanics of the critical state line at high stresses

John P. de Bono\*, Glenn R. McDowell

University of Nottingham, United Kingdom

## ARTICLE INFO

## Keywords:

Discrete element method  
DEM  
Particle crushing  
Critical state line  
State boundary surface

## ABSTRACT

A critical state line is presented for a crushable numerical soil, which is parallel to the isotropic normal compression line. A previous theory for the normal compression line, which correctly predicts the slope as a function of the size-effect on particle strength is extended to justify the slope of the critical state line. The micro mechanics behind critical states are examined, leading to a theory for a relationship between the volume of smallest particles and mean effective stress. A unique relationship exists for crushed states, leading to a two-dimensional interpretation of the state boundary surface for soils looser than critical.

## 1. Introduction

Following Pestana and Whittle [1], McDowell [2] proposed analytically that the high-stress normal compression line for a sand should be linear on  $\log e - \log \sigma$  axes. This was based on the kinematics of particle crushing and the assumption of a fractal particle size distribution. This was investigated numerically using the discrete element method [3], and it was found that the normal compression line (NCL) for a sand could be described by:

$$\log e = \log e_y - \frac{1}{2b} \log \frac{\sigma'}{\sigma'_y} \quad (1)$$

where  $e$  is the current voids ratio,  $\sigma'$  is the current stress,  $b$  describes the hardening rate of the particles, and  $e_y$  and  $\sigma'_y$  are constants defining the yield point. The parameter  $b$  defines the rate at which average particle strength increases with decreasing size:

$$\sigma_{av} \propto d^{-b} \quad (2)$$

and as shown by Eq. (1),  $b$  determines the slope ( $= 1/2b$ ) of the NCL on logarithmic axes. This compression law in Eq. (1) was tested against experimental data for which normal compression lines and particle strength data (i.e. values of  $b$ ) obtained from particle crushing tests were readily available in [4], and it was found to correctly predicted the slope of the NCL for each case.

It is a well-known phenomenon that the critical state line (CSL) for soils is parallel to the normal compression line [5,6], at least in conventional critical state soil mechanics. In this work, DEM simulations are used to establish a critical state line, and after ascertaining whether it is parallel with the NCL, to clarify what determines the slope and position of the CSL. In addition, we examine the micro mechanics

behind the CSL, in particular the co-ordination number and the importance of the 'smallest particles', which must be rigorously defined.

## 2. DEM model

The simulation results presented here were performed using the software PFC [7]. For computational efficiency all particles are modelled using spheres, and gravity is neglected. All simulations are performed using a cylindrical triaxial sample, enclosed vertically by rigid platens and laterally by a flexible, faceted cylindrical membrane, shown in Fig. 1. The membrane consists of 4320 facets and the vertices can move independently from one another. Essential simulation details are provided in Table 1. The initial sample (before isotropic compression) consists of approximately 700 randomly packed particles of 2 mm diameter; although the sample is compressed and crushed (generating greater quantities of smaller particles) before any shear tests are performed.

The work uses a simple crushing model and realistic particle strengths, which the authors have previously used to produce normal compression lines [3,8,9], which exhibit the same slope as observed experimentally for the sand. This crushing model uses the average octahedral shear stress as the particle fracture criterion:

$$q = \frac{1}{3} [(\sigma_1 - \sigma_2)^2 + (\sigma_2 - \sigma_3)^2 + (\sigma_1 - \sigma_3)^2]^{1/2} \quad (3)$$

which is calculated from the average principal stresses in a particle ( $\sigma_{1,2,3}$ ), in turn calculated from contacts with neighbouring bodies.

The strength data used here (and previously) is for a silica sand. From particle crushing tests [10], it was found that the size-effect on strength, i.e. the value of  $b$  in Eq. (2) was approximately 1 [10]. For a

\* Corresponding author.

E-mail address: [john.debono@nottingham.ac.uk](mailto:john.debono@nottingham.ac.uk) (J.P. de Bono).

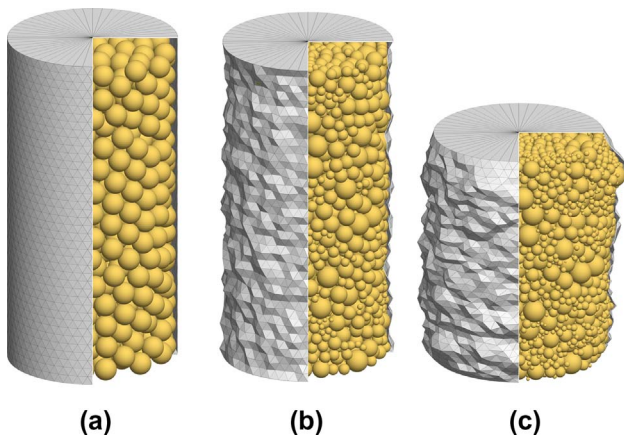


Fig. 1. Initial sample (a), after isotropic compression (b) and after shearing to critical state (c).

Table 1  
DEM properties.

General simulation properties	
Initial sample size: height × diameter (mm)	30 × 15
Initial no. of particles	723
Wall friction coefficient	0
Particle friction coefficient	0.5
Contact model	Hertz-Mindlin
Particle shear modulus (GPa)	28
Particle Poisson's ratio	0.25
Particle density (kg/m <sup>3</sup> )	2650
Damping coefficient	0.7
Initial voids ratio	0.75
Initial particle size (mm)	2
Weibull modulus	3.3
Initial particle strength, $q_{0,2}$ (MPa)	37.5

given size of particle, the strengths are distributed according to a Weibull distribution, defined by a characteristic value  $q_0$  and a modulus  $m$ . The strength  $q_0$  is a value such that 37% of particles of that size are stronger, and is numerically similar (and proportional) to the mean value. The modulus  $m$  defines the variability. For the silica sand, the modulus was found to be 3.3 [10]. The size-effect on strength for the simulations can therefore be written as:

$$q_0 \propto d^{-1} \tag{4}$$

where for example,  $q_0 = 37.5$  MPa for  $d = 2$  mm.

The particle breakage model replaces broken particles with 2 smaller fragments whilst obeying conservation of mass. The new fragments are placed within the boundary of the broken particle, aligned in the direction of the minor principal stress and therefore overlap. The fragments therefore move apart immediately following breakage (which requires a number of timesteps to be completed to allow energy dissipation, via friction and mechanical damping), details of which are given in [3], along with comparisons of alternative breakage models.

This initial sample is first isotropically compressed to establish a compression line, and shear tests are performed from various points along the loading path. The sample is also unloaded from different stresses, and further shear tests performed from along overconsolidated states.

During normal compression, the simulation proceeds by applying isotropic stress increments (100 kPa) using the wall servo-controls. Once a stress is applied, all particles are checked and allowed to break if their strength is exceeded. At this point a number of timesteps are completed to allow the overlapping fragments to move apart. If this breakage results in a drop in the applied isotropic pressure, then the stress increment is reapplied. Once a stress is sustainable without any

further breakages, the simulation progresses to the following increment.

The shear tests are strain-controlled. The upper platen is gradually accelerated (to 0.01 m/s) then decelerated, applying an axial strain increment of 0.1%. During this process the membrane servo-control acts to adjust the radial stress: the confining pressure is adjusted to ensure either constant  $\sigma_3$ ,  $p'$  or volume, depending on the stress path. Once the strain increment has been applied, particles are allowed to break, and the radial pressure is then reapplied if necessary. Once this process is complete, the subsequent strain increment is applied.

To enable the extensive number of simulations required in an acceptable timeframe, the initial sample contained only 723 particles (Fig. 1a). This is due to the crushing that occurs in nearly all shearing simulations, resulting in a wide range of sizes and much greater quantities of particles (Fig. 1c). A feature of the simulations is that there is no comminution limit—i.e. no lower limit to particle size. This allows the unadulterated evolution of a (fractal) particle size distribution. A consequence of this however is that the numerical timestep used in the simulations (influenced by  $d_{min}$ ) becomes very small. Thus, to enable the number of simulations required whilst not imposing artificial conditions, the initial number of particles is small, which helps minimise the calculation time once extensive crushing has occurred.

### 3. Simulation results

#### 3.1. Normal compression- and critical state lines

Isotropic compression results and two unloading lines from 20 and 30 MPa are presented in Fig. 2 on log  $e$ -log  $p'$  axes, also showing the points from which the shear tests were performed. From most of these points, 3 types of triaxial test were performed: constant- $\sigma_3$ , constant- $p'$ , constant-volume. However, it was not possible to perform constant-volume tests at the lowest  $p'$ , due to dry liquefaction (i.e. without pore fluid); and it was not computationally feasible to perform all of the constant- $\sigma_3$  and constant- $p'$  tests at the highest stresses due to extensive crushing caused by very large magnitudes of  $q$  and  $p'$ .

The critical states obtained from these tests are shown in Fig. 3. Triaxial simulations were run until reaching axial strains of between 25 and 35%, typically 30%, at which point all of the tests exhibited no (or in a few cases, negligible) volume or stress change. The ultimate states

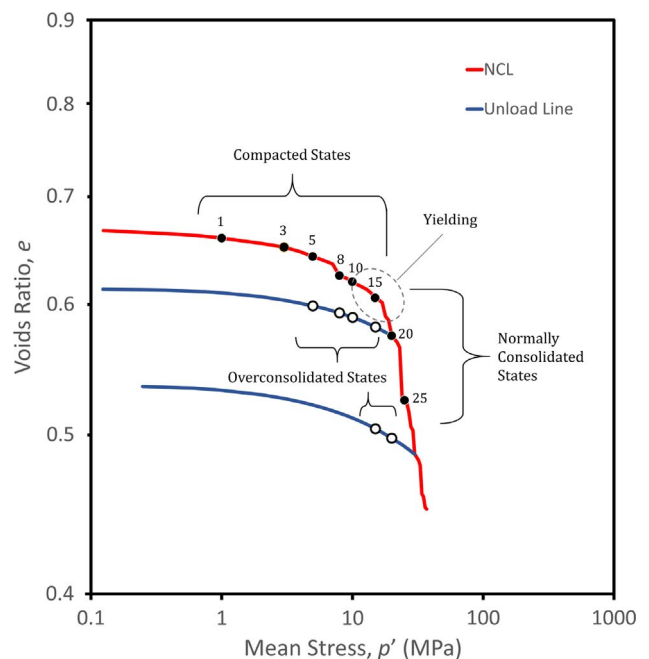


Fig. 2. Isotropic compression and unloading lines.

Download English Version:

<https://daneshyari.com/en/article/6709647>

Download Persian Version:

<https://daneshyari.com/article/6709647>

[Daneshyari.com](https://daneshyari.com)